

# The Fundamental Diagram of Pedestrian Movement Revisited

Armin Seyfried<sup>1</sup>, Bernhard Steffen<sup>1</sup>, Wolfram Klingsch<sup>2</sup> and Maik Boltes<sup>1</sup>

<sup>1</sup>Central Institute for Applied Mathematics, Research Centre Jülich, 52425 Jülich, Germany

<sup>2</sup>Institute for Building Material Technology and Fire Safety Science, University of Wuppertal  
Pauluskirchstrasse 7, 42285 Wuppertal, Germany

E-mail: A.Seyfried@fz-juelich.de, B.Steffen@fz-juelich.de, klingsch@uni-wuppertal.de, M.Boltes@fz-juelich.de

First subm. June 27, 2005; accepted September 12, 2005

## Abstract

The empirical relation between density and velocity of pedestrian movement is not completely analyzed, particularly with regard to the ‘microscopic’ causes which determine the relation at medium and high densities. The simplest system for the investigation of this dependency is the normal movement of pedestrians along a line (single-file movement). This article presents experimental results for this system under laboratory conditions and discusses the following observations: The data show a linear relation between the velocity and the inverse of the density, which can be regarded as the required length of one pedestrian to move. Furthermore we compare the results for the single-file movement with literature data for the movement in a plane. This comparison shows an unexpected conformance between the fundamental diagrams, indicating that lateral interference has negligible influence on the velocity-density relation at the density domain  $1 \text{ m}^{-2} < \rho < 5 \text{ m}^{-2}$ . In addition we test a procedure for automatic recording of pedestrian flow characteristics. We present preliminary results on measurement range and accuracy of this method.

**Keywords:** Traffic and crowd dynamics

## 1 Introduction

Pedestrian dynamics has a multitude of practical applications, like the evaluation of escape routes or the optimization of pedestrian facilities, along with some more theoretical questions [1, 2, 3, 4, 5, 6]. Empirical studies of pedestrian streams can be traced back to the year 1937 [6]. To this day a central problem is the relation between density and flow or velocity. This dependency is termed the fundamental diagram and has been the subject of many investigations from the very beginning [4, 6, 7, 8, 9, 10, 11, 12, 13, 14, 15, 16]. This relation quantifies the capacity of pedestrian facilities and thus allows e.g. the rating of escape routes. Furthermore, the fundamental diagram is used for the evaluation of models for pedestrian movement [17, 18, 19, 20], and is a primary test whether the model is suitable for the description of pedestrians streams [21, 22, 23, 24].

The velocity-density relation differs for various facilities like stairs, ramps, bottlenecks or halls. Moreover one has to distinguish between uni- or bi-directional streams. The simplest system in this enumeration is the uni-directional movement of pedestrians in a plane without bottlenecks. In this context the fundamental diagram of Weidmann [25] is frequently cited. It is a part of a review work and the author summarized 25 different investigations for the

determination of the fundamental diagram. Apart from the fact, that with growing density the velocity decreases, the relation shows a non-trivial form. Weidmann notes that different authors choose different approaches to fit their data, indicating that the dependency is not completely analyzed. A multitude of possible effects can be considered which may influence the dependency. For instance we refer to passing maneuvers, internal friction, self-organization phenomena or ordering phenomena like the ‘zipper’ effect [26]. A reduction of the degrees of freedom helps to restrict possible effects and allows an improved insight to the problem. To exclude in a natural way the influences of passing maneuvers, internal friction or ordering phenomena, we choose a one-dimensional system. At this we restrict the investigation on the velocity-density relation for the normal and not for the pushy or panic movement of pedestrians. Similar experiments with the focus on the time gap distribution and results for the clogging in pushy crowds can be found in [3].

Furthermore, we test a procedure for automatic recording of pedestrian flow characteristics. This method uses stereo video processing and allows the determination of trajectories of individual persons. We present preliminary results on measurement range and accuracy of this method.

## 2 Movement in a plane

In the field of pedestrian dynamics there are two different ways to quantify the capacity of pedestrian facilities. Either the relation between density  $\rho$  and velocity  $v$  or the relation between density and flow  $\Phi = \rho v$  is represented. Following Weidmann we choose the presentation of density and velocity.

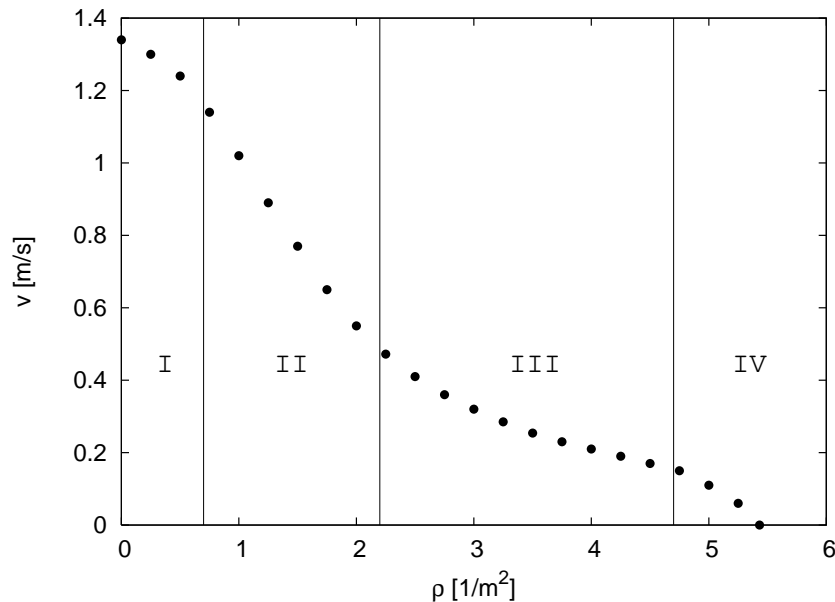


Figure 1: Empirical relation between density and velocity according to Weidmann (Page 52 in [25]). The partition refers to domains with qualitative different decrease of the velocity.

Figure 1 shows the empirical velocity-density relation for pedestrian movement in a plane

according to Weidmann<sup>1</sup>. The maximal density in this diagram is  $5.4/m^2$ , though some authors [6, 7, 12] have found higher densities. The slope varies for different density-domains indicating diverse effects which reduce the velocity. We discuss possible causes for this slope-variation by means of the Level of Service concept (LOS) [4, 5, 25].

**Domain I**  $\rho < 0.7$  At low densities there is a small and increasing decline of the velocity. The velocity is mostly determined by the individual free velocity of the pedestrians. Passing maneuvers for keeping the desired velocity are possible. The decrease is caused by the passing maneuvers.

**Domain II**  $0.7 \leq \rho < 2.3$  The velocity decrease is nearly linear with growing density. Due to the reduction of the available space, passing maneuvers of slower pedestrians are hardly feasible and the possibility to choose the desired velocity is restricted. At least at uni-directional streams the available space is large enough to avoid contacts with other pedestrians. Thus the internal friction can only be of negligible influence.

**Domain III**  $2.3 \leq \rho < 4.7$  The linear decrease of the velocity ends and the curvature changes. For growing density the velocity remains nearly constant. Contacts with other pedestrians are hardly avoidable. While the internal friction increases compared with domain II, the reduction of the velocity diminishes.

**Domain IV**  $\rho \geq 4.7$  The velocity declines rapidly. The available space is strongly restricted. Internal friction may be a determining factor. There has to be a maximal density because the pedestrians behave like hard bodies.

As pointed out, there are several hints to effects which can influence the reduction of the velocity at different densities. But it is not clear which ‘microscopic’ properties of pedestrian movement lead to the nearly linear decrease of the velocity and to a slower decrease at high densities. Particularly the possible influence of the internal friction is contradictory to the slope of the velocity-density relation. We have to clarify the influences of collective behavior like marching in lock-step [10] or self-organization phenomena like the ‘zipper’ effect, which can be observed at bottlenecks [26].

### 3 Single-file movement

#### 3.1 Description of the experiment

Our target is the measurement of the relation between density and velocity for the single-file movement of pedestrians. To facilitate this with a limited amount of test persons also for high densities and without boundary effects, we choose a experimental set-up similar to the set-up in [8].

The corridor, see Figure 2, is build up with chairs and ropes. The width of the passageway in the measurement section is  $0.8m$ . Thus passing is prevented and the single-file movement is enforced. The width of the corridor is not important as long it does not impede the free movement of the arms and on the other hand does not allow the formation of two - possible interleaving - lanes. The circular guiding of the passageway gives periodic boundary

---

<sup>1</sup>Note that Weidmann’s combination does not distinguish between uni- (e.g. [8]) and bi-directional (e.g. [9]) movement

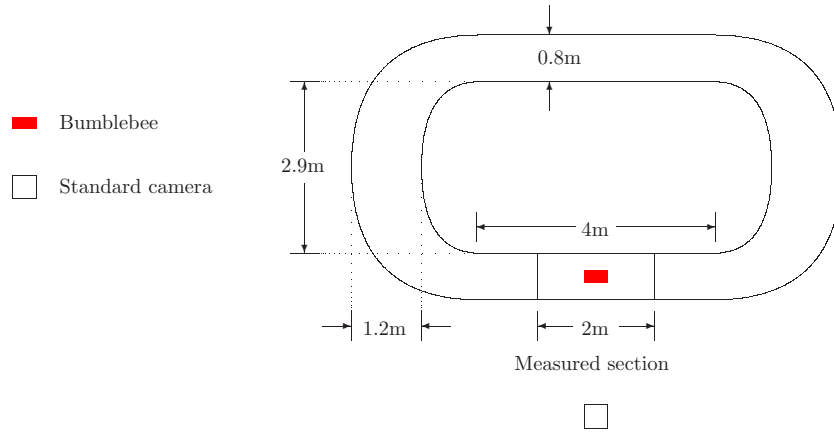


Figure 2: Experimental set-up for the measurement of the velocity-density relation for the single-file movement.

conditions. To reduce the effects of the curves on the measurement, we broaden the corridor in the curve and choose the position of the measured section in the center of the straight part of the passageway. The length of the measured section is  $l_m = 2\text{ m}$  and the whole corridor is  $l_p = 17.3\text{ m}$ . The experiment is located in the auditorium Rotunde at the Central Institute for Applied Mathematics (ZAM) of the Research Centre Jülich. The group of test persons is composed of students of Technomathematics and staff of ZAM. To get a normal and not a pushy movement the test persons are instructed not to hurry and omit passing. This results in a rather relaxed conduct, i. e. the resulting free velocities are rather low. Most real life situations will show higher free velocities and more pushing. To enable measurements at different densities we execute six cycles with  $N = 1, 15, 20, 25, 30, 34$  numbers of test persons in the passageway. For the cycle with  $N = 1$  every person passes alone through the corridor. For the other cycles we first distribute the persons uniformly in the corridor. After the instruction to get going, every person passes the passageway two to three times. After that we open the passageway and let the test persons get out. We observed that the test persons walked straight through the measurement section and follow each other up to a few centimeter of lateral variation. This does not mean that they walked exactly on the same path but lateral fluctuations are highly correlated. This observation is reinforced by the documentation of marching in lock-steps, which will be discussed later.

### 3.2 Measurement set-up

For the measurement of the flow characteristics we use both a manual and an automatic procedure. The manual procedure is based on standard video recordings with a DV camera (PAL format, 25 fps) of the measured section. These recordings are prepared on a computer to show time, frame number and the limits of the measured section. After the preparation the recordings were analyzed frame-wise, thus the accuracy of the extracted time is  $0.04\text{ s}$ . To minimize the errors for extracting time data, the collected time is transferred by cut and paste between the video editing system and the spread sheet. Figure 3 shows one frame of the cycle with  $N = 20$  persons. For every test person  $i$  we collect the entrance time (of the ear) in the measurement section  $t_i^{in}$  and the exit time  $t_i^{out}$ . To ease the assignment of times the test persons carry numbers.

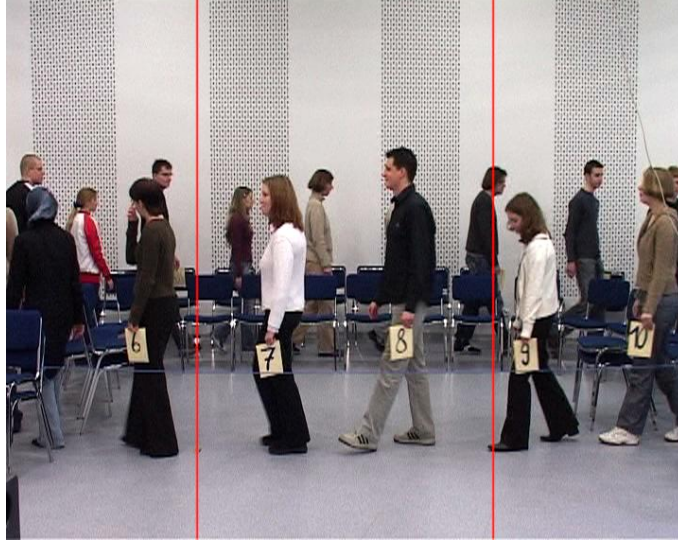


Figure 3: One frame of the standard video recording of the cycle with  $N = 20$  after the preparation for the manual analysis.

Additionally we test an automated procedure, based on a commercial system of Point Grey Research [27]. The system is composed of the Bumblebee stereo vision camera and the software packages Digidlops, Triclops and Censys3d. The software uses stereo recordings for detection and tracking of peoples. The resulting trajectories allow the analysis of pedestrian movement in space and time. For this measurement we use a bumblebee BW-BB-20. The analysis device is an IBM ThinkPad T30 with an Intel Pentium 4 Mobile CPU (512 MB RAM) and the operating system WIN XP SP1. The data transfer from the camera to the analysis device is realized via FireWire and a PCMCIA FireWire card. Following the recommendation of the manufactures we decide to process the data directly without storing the pictures on a hard disk. In our measurement setup we are bounded on a transfer rate to the analysis device of about 2 times 20 fps with a resolution of 320 x 240 pixels.

### 3.3 Data analysis

The manual analysis uses the entrance and exit times  $t_i^{in}$  and  $t_i^{out}$ . These two times allow the calculation of the individual velocities  $v_i^{man} = l_m / (t_i^{out} - t_i^{in})$  and the momentary number  $n(t)$  of persons at time  $t$  in the measured section. The concept of a momentary ‘density’ in the measurement region is problematic because of the small (1-5) number of persons involved.  $\tilde{\rho}^{man}(t) = n(t)/l_m$  jumps between discrete values. For a better definition we choose  $\rho^{man}(t) = \sum_{i=1}^N \Theta_i(t)/l_m$ , where  $\Theta_i(t)$  gives the ‘fraction’ to which the space between person  $i$  and person  $i + 1$  is inside.

$$\Theta_i(t) = \begin{cases} \frac{t - t_i^{in}}{t_{i+1}^{in} - t_i^{in}} & : t \in [t_i^{in}, t_{i+1}^{in}] \\ 1 & : t \in [t_{i+1}^{in}, t_i^{out}] \\ \frac{t_{i+1}^{out} - t}{t_{i+1}^{out} - t_i^{out}} & : t \in [t_i^{out}, t_{i+1}^{out}] \\ 0 & : \text{otherwise} \end{cases} \quad (1)$$

In Figure 3 the ‘fractions’ are  $\Theta_6(t) \approx 0.6$ ,  $\Theta_7(t) = 1$ ,  $\Theta_8(t) \approx 0.8$ ,  $\Theta_9(t) = 0$ , resulting in  $\rho(t) \approx 1.2 m^{-1}$ . This is 3 persons per  $2.5 m$ , which is about the distance between person number 6 and number 9. The time average of  $\tilde{\rho}^{man}$  and  $\rho^{man}$  is almost the same.

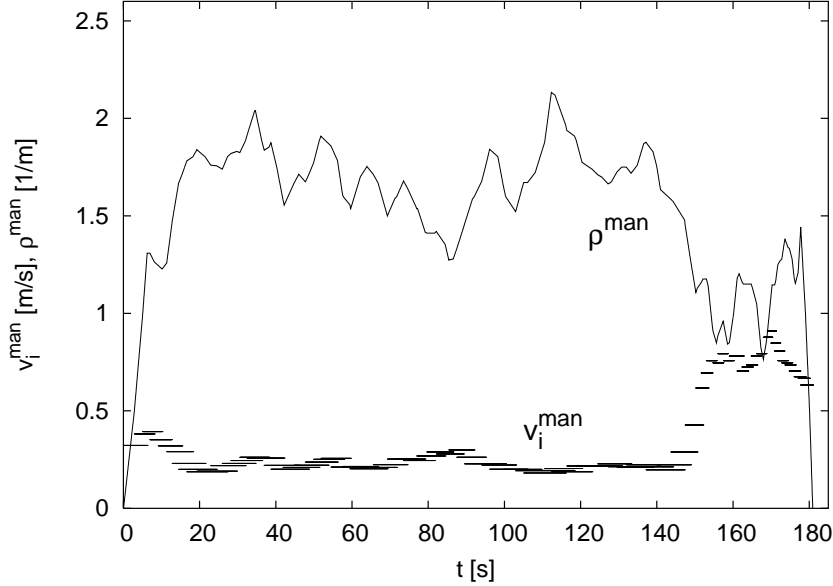


Figure 4: Time development of the density and individual velocities for the cycle with  $N = 30$ . The upper line shows the density, the lower bars label the time-slots in which the pedestrian  $i$  is in the measured section and the associated mean velocity  $v_i$ . The fluctuations of the individual velocities are correlated with the density. We see the influence of the starting phase and the rearrangement of the boundary conditions due to the opening of the passageway at the end of the cycle.

Figure 4 shows the development of the density and velocity of individual persons in time. At the beginning the pedestrians do not react simultaneously and they have to tune their movement. After the tuning phase one sees slow moderate size fluctuations of the density and the velocity. It becomes obvious that these ‘microscopic’ fluctuations are correlated. After the opening of the passageway the density declines and as a consequence the velocity grows. To consider this correlation in the analysis we regard a crossing of an individual pedestrian  $i$  with velocity  $v_i^{man}$  as one statistical event, which is associated to the density  $\rho_i^{man}$ . While  $\rho_i^{man}$  is the mean value of the density during the time-slice  $[t_i^{in}, t_i^{out}]$ . For this analysis we exclude the part of the data where the influence of the tuning phase and the rearrangement of the boundary conditions is explicit.

Figure 5 shows the distribution of the events  $(v_i^{man}, \rho_i^{man})$  of the cycles with  $N = 15, 20, 25, 30$  and  $34$ . The cycles with  $N = 15, 20$  and  $25$  result in clearly separated areas of densities and velocities. These areas blend for the cycles with  $N = 30$  and  $34$ .

The automated procedure uses the trajectories for the analysis. The accuracy of the trajectory measurement depends on many factors, like the size of the covered area, the capability of the analysis device and the settings of parameters in software Censys3d for people detection and tracking. In test-runs we optimize these parameters for normal and not too crowded conditions. But during the experiment we realized that the system is too sensitive and with

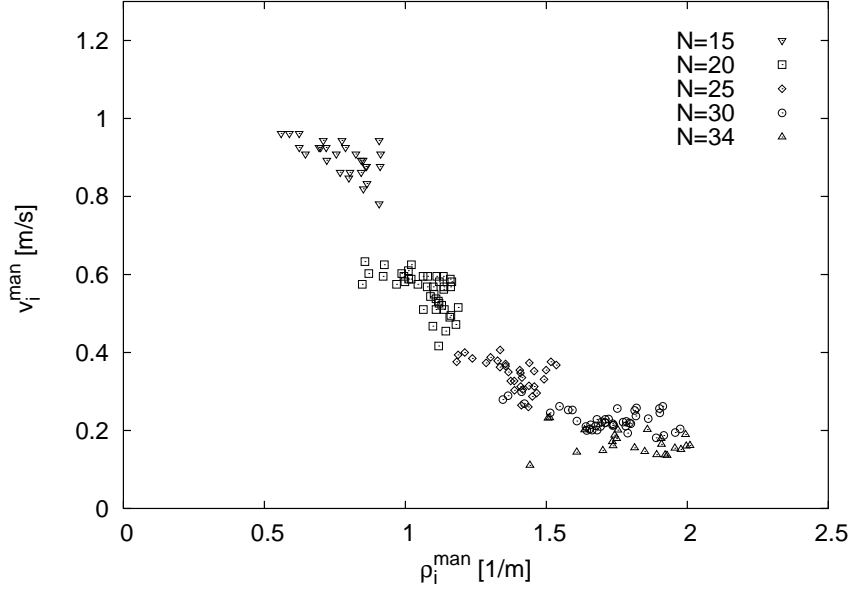


Figure 5: Dependency between the individual velocity and density for the cycles with  $N = 15, 20, 25, 30$  and  $34$ .

growing density the mismeasurements increase. For example we observe the loss of trajectories or persons with two trajectories, see figure 6. Due to the mismeasurements the determination of densities or other microscopic values like the distance between the pedestrians is not reliable. The resulting trajectories are thus only appropriate for the calculation of the mean value of the velocity. For this purpose we determine for every crossing pedestrian  $i$  the first  $(x_i^f, t_i^f)$  and the last point  $(x_i^l, t_i^l)$  of the trajectory in the measured section and calculate the velocity through  $v_i^{aut} = (x_i^l - x_i^f)/(t_i^l - t_i^f)$ .

In the next step we test if the mismeasurements lead to systematic errors in the determination of the velocities and cross-check the data from the manual analysis. For this we exclude the data where the influence of the starting phase and opening of the passageway are apparent. To reduce the influence of mismeasurements we take into account only these trajectories, which last for at least one second.

For the test we determined the following values. Based on the individual velocities  $v_i^{aut}$  and  $v_i^{man}$  we calculate the mean value  $v^{man}$  and  $v^{aut}$  over all individual velocities for the different cycles. Furthermore we determine the mean value of the density  $\rho^{man}$  during one cycle based on the manual analysis and compare them with the densities calculated through  $\rho = N/l_p$ , where  $l_p$  is the length of the passageway. The values are summarized in the following table. Aside from local fluctuations, possible reasons for the deviations of the densities  $\rho^{man}$  and  $\rho$  are the influence of the curve and the broadening of the passageway in the curve. The mean velocities calculated automatically agree roughly with the velocities extracted from the manual procedure. We get a very good agreement for medium densities  $N = 15, 20$ . Notable deviations arise at high velocities and high densities. The mismeasurements caused by loosing and picking up of trajectories increase the fluctuations ( $\sigma$ ). The deviation of the mean value for the cycle with  $N = 1$  from the literature value  $v_{free} = 1.34 m/s$  according to Weidmann, can be explained by the instruction to the test persons not to hurry.

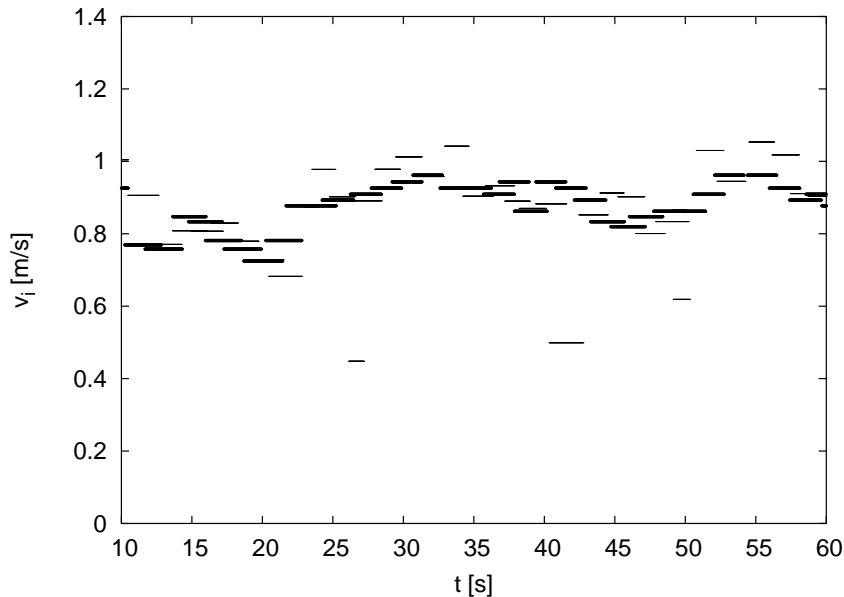


Figure 6: Comparison for the cycle with  $N = 15$ . The thick lines represent the time-slots and velocity determined through the manual procedure. The thin lines results from the trajectories gained by the automated procedure. The values for the velocities agree roughly, but the results are not comparable on a microscopic level.

## 4 Results

In the following we focus on the distance between the pedestrians. For the single-file movement the distance to the next close-by pedestrian can be regarded as the required length  $d$  of one pedestrian to move with velocity  $v$ . Considering that in a one-dimensional system the harmonic average of this quantity is the inverse of the density,  $d = 1/\rho$ , one can investigate the relation between required length and velocity by means of the velocity-density relation for the single-file movement.

Figure 7 shows the dependency between required length and velocity. We tested several approaches for the function  $d = d(v)$  and found that a linear relationship with  $d = 0.36 + 1.06 v$  gives the best fit to the data. According to [25] the step length is a linear function of the velocity<sup>2</sup> only for  $v \geq \approx 0.5 m/s$ . Thus it is surprising, that the linearity for entire distance holds even and persists for velocities smaller than  $0.5 m/s$ . Possible explanations will be discussed later.

To compare the relation between velocity and density of the single-file movement ( $1d$ ) with the movement in a plane ( $2d$ ), we have to transform the line-density to a area-density.

$$\rho_{1d \rightarrow 2d} = \rho_{1d}/c(v) \quad c(v) = \alpha + \beta v \quad (2)$$

The correction term  $c(v)$  is introduced to take into account that the lateral required width is as well as the longitudinal required length  $d$  a function of the velocity. For a first approximation we assume a linear dependency. According to [25] the mean value of the width of the human

<sup>2</sup>Lower average velocities arise from a lower step frequency.



$N$	$\rho[1/m]$	$\rho^{man}[1/m]$	$v^{man}[m/s]$	$v^{aut}[m/s]$
1			1.24 (0.15)	1.37 (0.21)
15	0.87	0.77 (0.12)	0.90 (0.05)	0.88 (0.15)
20	1.16	1.07 (0.11)	0.56 (0.05)	0.51 (0.11)
25	1.45	1.39 (0.12)	0.35 (0.04)	0.26 (0.14)
30	1.73	1.71 (0.17)	0.23 (0.03)	0.16 (0.15)
34	1.97	1.76 (0.24)	0.17 (0.03)	0.13 (0.34)

Table 1: Comparison of mean values and standard deviations ( $\sigma$ ) gained from the automated and manual procedure.

body is  $0.46 m$  and thus we set  $\alpha = 0.46 m$ . The parameter  $\beta$  considers that with increasing velocity the lateral required width grows.

The comparison of the relation between velocity and density for the single-file movement with the movement in a plane according to Weidmann shows a surprising conformity, see Figure 8. So far the value of  $\beta$  is unknown, but the figure shows, that for a large domain of reasonable values we have an obvious accordance between the fundamental diagrams. For the lower bound of  $\beta = 0.05 s$  one gets a lateral required width at  $v = 1.3 m/s$  of  $c = 0.5 m$ , which is to definitely too small. For the upper bound we choose  $\beta = 0.3 s$  which results in  $c(1.3 m/s) = 0.9 m$  which is certainly too high. But it becomes apparent, that the qualitative shape of the velocity-density relations and the magnitude of the velocities agree between the upper and the lower bound of  $\beta$ . This conformance indicates that two-dimensional specific properties, like internal friction and other lateral interferences, have no strong influence on the fundamental diagram at least at the density domains considered.

Instead, the visual analysis of the video recordings suggests that the following ‘microscopic’ properties of pedestrian movement determine the relation between velocity and density. At intermediate densities and velocities the step length is reduced with increasing density. The distance to the pedestrian in front is related to the step length as well as to the safety margin to avoid contacts with the pedestrian in front. Both, step length and safety margin are connected with the velocity. At high densities and small velocities we observed that small groups pass into marching in lock-step, see Figure 9. Furthermore the utilization of the available place is optimized. This is achieved by some persons setting their feet far right and left of the line of movement, giving some overlap in the space occupied with the pedestrian in front. While at intermediate densities and relative high velocities the pedestrians are concentrated on their movement, this concentration is reduced at smaller velocities and leads to a delayed reaction on the movement of the pedestrian in front. The marching in lock-steps and the optimized utilization of the available space, which compensate the slower step frequency, are possible explanation that the linearity between the required length and the velocity holds even, see Figure 7.

## 5 Summary and outlook

In the investigation presented we determine the fundamental diagram for the single-file movement of pedestrians under laboratory conditions. The data are appropriate to test, if microscopic models are able to reproduce the empirical relation between velocity and density in

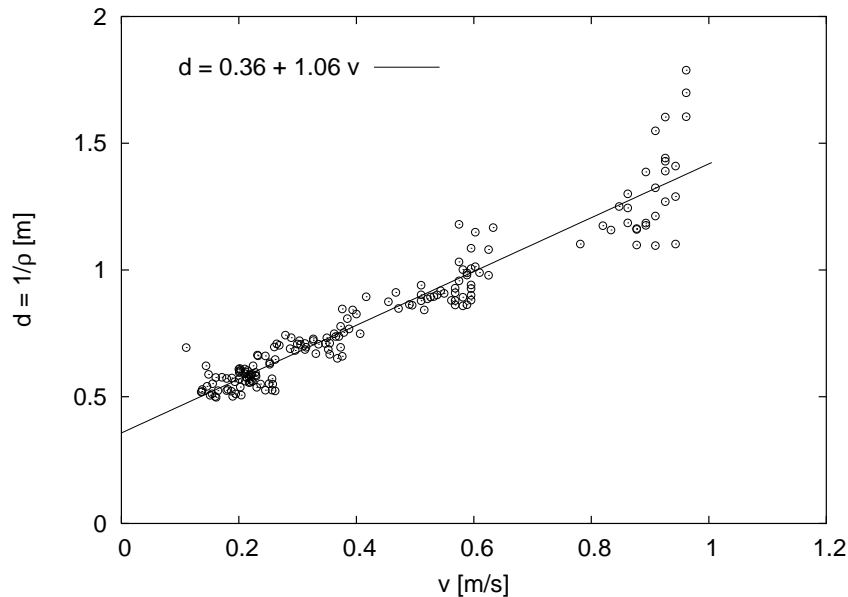


Figure 7: Dependency between required length and velocity according to the data from the cycles with  $N = 15, 20, 25, 30$  and  $34$ . We found that a linear relationship gives the best fit to the data.

the simplest system.

The test of the automated procedure shows that this method is in principle capable to measure characteristics of pedestrian movement. The mean values of the velocities for different densities acquired automatically are comparable with those of the manual data analysis. To facilitate the measurement of microscopic characteristics we plan to increase the resolution of the stereo recordings and the transfer rate to the analysis system.

The comparison of the velocity-density relation for the single-file movement with the literature-data for the movement in a plane shows a surprising agreement for  $1 \text{ m}^{-2} < \rho < 5 \text{ m}^{-2}$ . The conformance indicates that the internal friction and other lateral interferences, which are excluded in the single-file movement, have no influence on the relation at the density domains considered. The visual analysis of the video recording give hints to possible effects, like the self-organization through marching in lock-step, the optimized utilization of the available space at low velocities and the velocity dependence of step-length and safety margin. The investigation of the dependency between the required length of one pedestrian and velocity indicates a linear relation. For the domain  $0.1 \text{ m/s} < v < 1.0 \text{ m/s}$  we obtain  $d = 0.36 + 1.06 v$ . The investigation of the interplay between the self-organization effects and required length and thus a detailed quantification of these effects is necessary.

For real life situation including bottlenecks and changes in direction, and for higher densities, however, two-dimensional effects can certainly not be disregarded. Moreover, for most laboratory experiments, the emotional situation of the participants is relaxed, so some effects of real life will not be shown, as already observed in [28]. Further studies will be required, and some of these will be vastly easier after the improvement of the automated procedure.

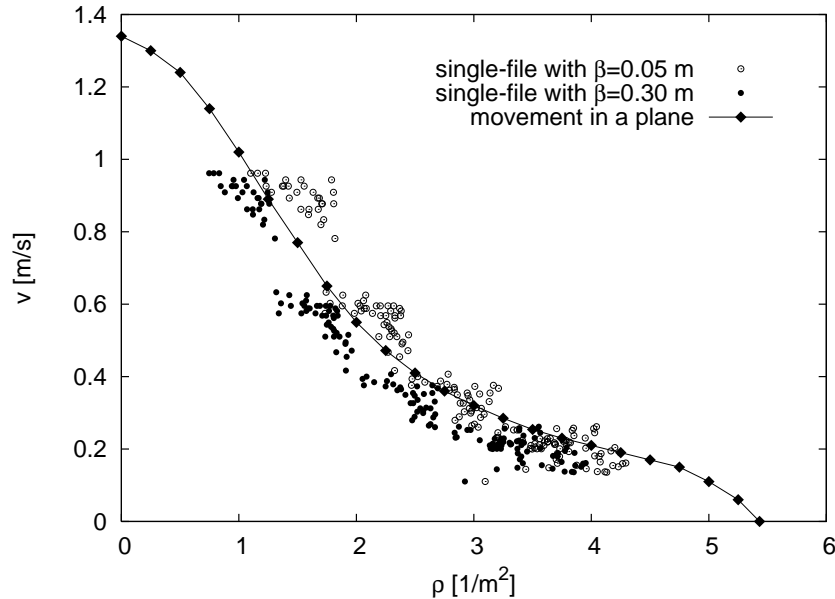


Figure 8: Comparison of the velocity-density relation for the single-file movement with the movement in a plane according to Weidmann [25]. For the scaling of the line-density we choose  $\beta = 0.05$  s and  $\beta = 0.3$  s, see Equation 2.

### Acknowledgments

We thank Patrick Hartzsch for extracting the times from the video, Dr. Wolfgang Meyer for the advice with statistics, Oliver Passon for careful reading and Thomas Lippert for discussions.

### References

- [1] Schreckenberg M and Sharma S D (eds), 2001 Pedestrian and Evacuation Dynamics (Springer, Berlin)
- [2] Galea E R (ed.), 2003 Pedestrian and Evacuation Dynamics (CMS Press, London)
- [3] Helbing D, Buzna L, Johansson A, and Werner T, Self-organized pedestrian crowd dynamics: Experiments, simulations, and design solutions, 2005 Transp. Sci 39 1
- [4] Oeding D, 1963 Verkehrsbelastung und Dimensionierung von Gehwegen und anderen Anlagen des Fußgängerverkehrs, Straßenbau und Straßenverkehrstechnik 22 (Bundesministerium für Verkehr, Abt. Straßenbau, Bonn)
- [5] Fruin J J, 1971 Pedestrian Planning and Design (Elevator World, New York)
- [6] Predtetschenski W M and Milinski A I, 1971 Personenströme in Gebäuden - Berechnungsmethoden für die Projektierung (Verlagsgesellschaft Rudolf Müller, Köln-Braunsfeld)
- [7] Togawa K, Study on fire escapes basing on the observation of multitude currents, 1955 Report of the Building Research Institute 14 1 (in Japanese)
- [8] Hankin B D and Wright R A, Passenger flow in subways, 1958 Operational Research Quarterly 9 81

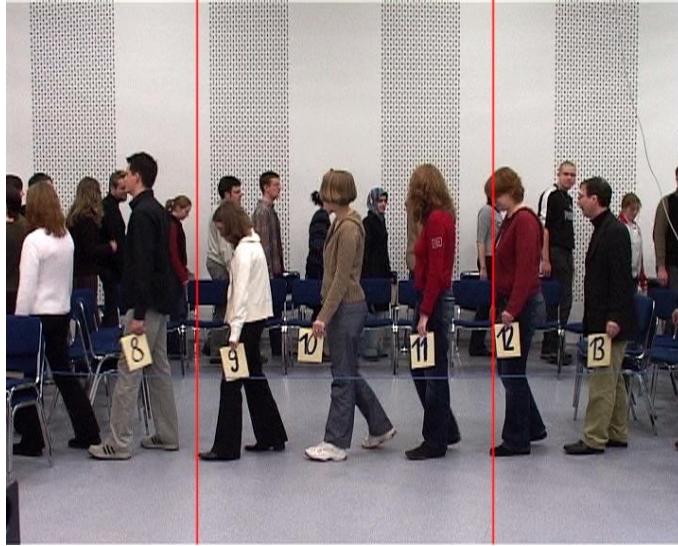


Figure 9: Example for marching in lock-step for the cycle with  $N = 30$ .

- [9] Older S J, Movement of pedestrians on footways in shopping streets, 1968 Traf. Engin.+Cont. 10 160
- [10] Navin P D and Wheeler R J, Pedestrian flow characteristics, 1969 Traf. Engin. 39 31
- [11] Carstens R L and Ring S L, Pedestrian capacities of shelter entrances, 1970 Traf. Engin. 41 38
- [12] Westphal J, 1971 Untersuchung von Fussgängerbewegungen auf Bahnhöfen mit starkem Nahverkehr, Wissenschaftliche Arbeiten 2 (Dissertation Technischen Universität Hannover)
- [13] O'Flaherty C A and Parkinson M H, Movement in a city centre footway, 1972 Traf. Engin.+Control Feb. 434
- [14] Polus A, Joseph J L and Ushpiz A, Pedestrian flow and level of service, 1983 J. Transp. Engin. 109 46
- [15] Lam W H K, Morrall J F and Ho H, Pedestrian flow characteristics in Hong Kong, 1995 Transp. Res. Rec. 1487 56
- [16] Hoskin K J and Spearpoint M, Crowd characteristics and egress at stadia, 2004 Proceedings of the third International Symposium on Human Behaviour in Fire (London)
- [17] Helbing D and Molnár P, Social force model for pedestrian dynamics, 1995 Phys. Rev. E 51 4282
- [18] Burstedde C, Klauck K, Schadschneider A and Zittartz J, Simulation of pedestrian dynamics using a two-dimensional cellular automaton, 2001 Physica A 295 507
- [19] Keßel A, Klüpfel H, Wahle J and Schreckenberg M, Microscopic simulation of pedestrian crowd motion, in [1]
- [20] Hoogendoorn S P and Bovy P H L, Gas-kinetic modeling and simulation of pedestrian flows, 2000 Transp. Res. Rec. 1710 28
- [21] Hoogendoorn S P, Bovy P H L and Daamen W, Microscopic pedestrian wayfinding and dynamics modelling, in [1]

- [22] Meyer-König T, H. Klüpfel and M. Schreckenberg, Assessment and analysis of evacuation processes on passenger ships by microscopic simulation, in [1]
- [23] Kirchner A, Klüpfel H, Nishinari K, Schadschneider A and Schreckenberg M, Discretization effects and the influence of walking speed in cellular automata models for pedestrian dynamics, 2004 J. Stat. Mech. 10011
- [24] [www.rimea.de](http://www.rimea.de)
- [25] Weidmann U, Transporttechnik der Fußgänger, 1993 Schriftenreihe des IVT Nr. 90, zweite ergänzte Auflage (ETH Zürich)
- [26] Hoogendoorn S P and Daamen W, Pedestrian behavior at bottlenecks, 2005 Transp. Sci. 39 0147
- [27] [www.ptgrey.com](http://www.ptgrey.com)
- [28] Koshi M, Iwasaki M and Ohkura I, Some findings and an overview on vehicular flow characteristics, 1983 Proceedings of the 8th International Symposium on Transportation and Traffic Flow Theory (Toronto, Ontario)